Carbonates and Evaporites (2020) 35:43
https://doi.org/10.1007/s13146-020-00573-w

ORIGINAL ARTICLE

Depositional sequences and microfacies of Lower Carboniferous strata in the Marsel block of the Chu-Sarysu Basin, Southern Kazakhstan

Yuan Wang[1,2] · Changsong Lin[3] · Yanda Sun[4] · Jingyan Liu[5] · Hao Li[3] · Haiquan He[4] · Qinglong Wang[4] · Muye Ji[3] · Manli Zhang[3] · Bozhi Zhao[3] · Zhiyuan Zhang[5]

Accepted: 25 February 2020 / Published online: 18 March 2020

Abstract

The sequence development and evolution of Lower Carboniferous strata in the Marsel block of the Chu-Sarysu Basin, Kazakhstan have been established through detailed sedimentological analysis of cores, petrophysical data, and new seismic interpretations. Four depositional sequences and eighteen parasequences were classified in the Lower Carboniferous strata. Each depositional sequence is composed of a transgressive systems tract (TST) and highstand systems tract (HST), roughly coinciding, respectively, with the following four stratigraphic intervals (1) lower Tournaisian (C_1t) through lower Visean (C_1v-1) strata; (2) middle Visean (C_1v-2) strata; (3) upper Visean (C_1v-3) strata; and (4) Serpukhovian (C_1sr) strata. Parasequences are bounded by an instantaneous drowned punctuated surface (C_1t and C_1v) or instantaneous exposed punctuated surface (C_1sr). In addition, petrographic studies have led to the recognition of 20 microfacies, distributed on the major depositional facies zones of the outer ramp (Mf1, Mf6, Mf20), middle ramp (Mf3–5, Mf8–13), and inner ramp (Mf2, Mf4, Mf7, Mf9, Mf12, Mf14–19). They are grouped into seven facies associations corresponding to widespread deposits of tidal flats (MA3, MA5), shallow shoals (MA6), and shallow lagoons (MA4) in the inner ramp; deposits of restricted lagoons (MA1) and local patch shoals (MA7) in the middle ramp and a relatively small outer ramp deposits (MA2). SQSQ All the microfacies and their associations are grouped into the following 6 major facies belts: outer ramp; restricted lagoon, and patch shoals in the middle ramp; and shallow shoals, restricted lagoon, subtidal to intertidal and supratidal in the inner ramp. The interpretation of these facies belts suggests a shallow warm-water tropical-subtropical depositional environment on a passive continental margin ramp. Facies correlation between wells in sequence framework suggests that the strata may be divided into four sequences (SQ1, SQ2, SQ3, SQ4). SQ1 and SQ2 are dominated by lagoon facies and outer ramp facies in the northwest area in the TST, and tidal flat facies in the HST; SQ3 is characterized by restricted to semi-restricted lagoon facies in the TST and local patch shoal facies and mixed tidal flat facies in the HST; SQ4 is marked by restricted lagoon facies in the TST and evaporitic lagoon, tidal flat, and shallow shoal facies in the HST. The research results can be used for investigating the development and distribution of potential reservoirs in the Lower Carboniferous strata of the Chu-Sarysu Basin; the reservoirs in the HST of late Visean and Serpukhovian in the northern and southeastern part of the platform interiors may be of premium quality.

Keywords Lower Carboniferous · Sequence stratigraphy · Carbonate microfacies · Marsel block · Chu-Sarysu basin · Southern Kazakhstan

Introduction

The northwest-to-southeast-trending Chu-Sarysu Basin, covering a very large area of more than 14.7×10^4 km^2, is located in the southern part of the Republic of Kazakhstan (Fig. 1a). The basin is one of the five commercial petroleum-bearing basins in Kazakhstan (Zheng et al. 2009) with fourteen gas fields discovered (Effimoff 2001; Pang et al. 2014), the recoverable reserves of which have reached 254.8×10^8 m^3 (Pang 2016). The upper Paleozoic reservoirs in this basin yield great potential for gas production, especially in the following gas-bearing zones: (1) the southern border of the Kokpansor Depression (Fig. 1b), where the Pridorozhnoye, Tamgalytar, Ortalyk and Western Oppak

✉ Yuan Wang
1370051652@qq.com

Extended author information available on the last page of the article

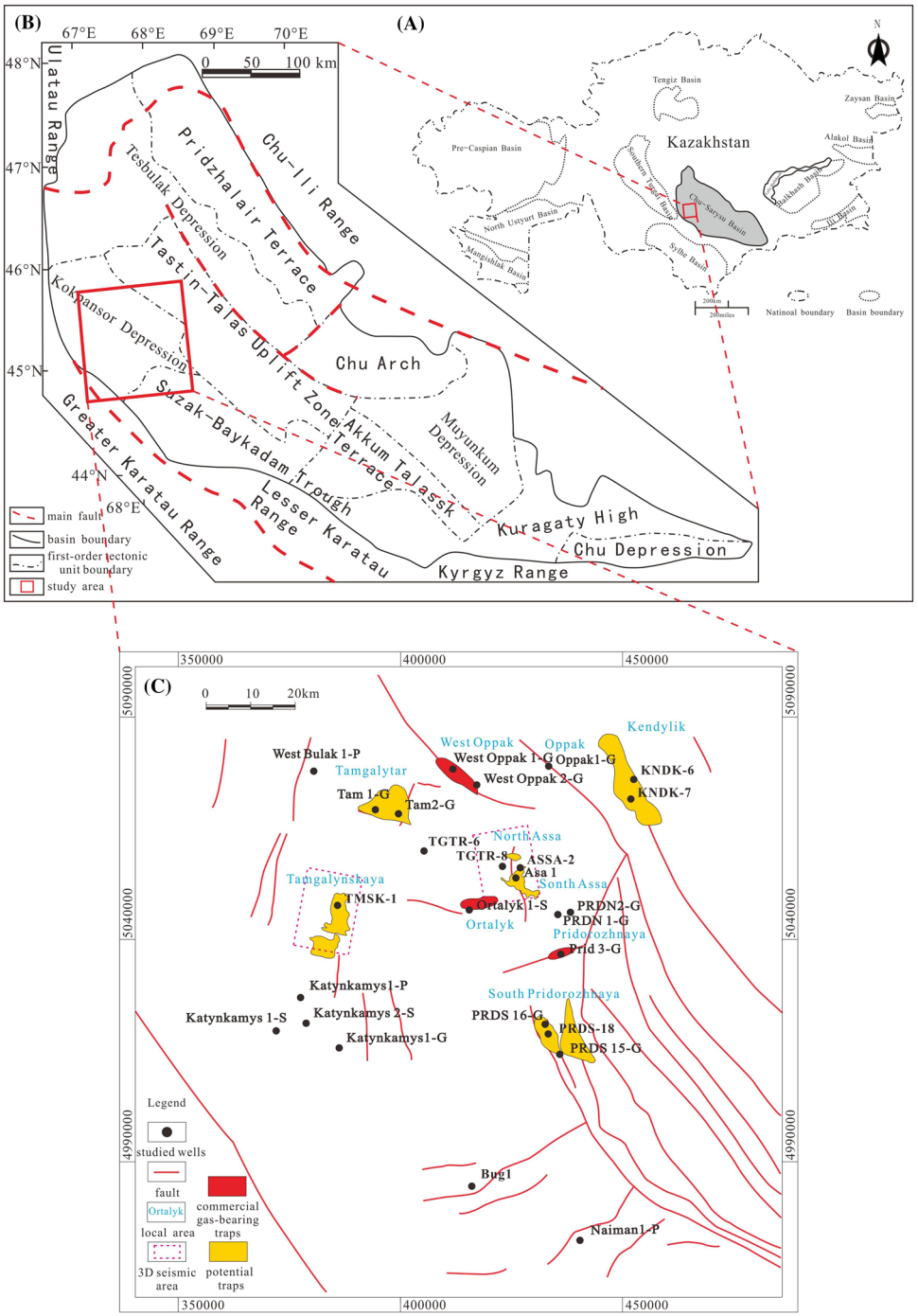

Fig. 1 Location of the study area in Southern Kazakhstan

fields are located, and (2) the northern part of the Moinkum Depression, where the Amangeldy, Airakty, Zharkum, Maldybai fields are located (Fig. 1c). Previous studies of the basin have investigated the cyclicity of Lower Carboniferous gas-producing strata and oil potential in relation to tectonic movements (Sinitsyn 1991; Sokolova 1974), evaluated oil and gas prospects in middle and upper Paleozoic strata (Sokolov et al. 1979), predicted petroleum accumulation in Lower Carboniferous fractured reservoirs in the west and northwest parts of the basin, as well as Lower Carboniferous reservoirs in the east part of the Kokpansor depression (Li and Filip'Yev 1982). The results show that Lower Carboniferous strata of the Chu-Sarysu Basin are favorable exploration targets for gas.

The Marsel block, located in the north of the Chu-Sarysu Basin, has an area of $1.85 \times 10^4 km^2$ and includes both the Kokpansor Depression and the northern Suzak-Baykodau Depression. (Fig. 1b). Oil and gas prospecting during the

1970s led to the discovery of commercial-grade oil and gas deposits from upper Paleozoic reservoirs in the Pridorozhnoe, West Oppak, Tamgalytar and Ortalyk uplifts in the Marsel block (Fig. 1c). The study area contains Lower Carboniferous carbonate platform deposits that accumulated on a passive continental margin. These carbonate deposits are regarded as a second-order sequence that may be subdivided into four third-order sequences composed of transgressive system tracts and highstand system tracts. The four third-order sequences are roughly correlated with the following four stratigraphic intervals delineated by Pang et al. (2014) and Xu et al. (2014): (1) lower Tournaisian (C_1t) through lower Visean (C_1v-1) strata; (2) middle Visean (C_1v-2) strata; (3) upper Visean (C_1v-3) strata; and (4) Serpukhovian (C_1sr) strata. Major early Carboniferous sedimentary facies in the Marsel block include evaporative carbonate platform deposits, open platform reef and shoal deposits, platform margin reef and shoal deposits, restricted platform evaporite deposits, restricted platform inter-shoal and shallow lagoon deposits, and drowned rimmed carbonate platform deposits (Xu et al 2014). However, despite these research results, detailed depositional sequences and microfacies of the Lower Carboniferous strata in the Marsel block have not been systematically studied due to the inadequacy of data from cores and geophysical logs. Thus, further exploration of potential hydrocarbon reservoirs in the Lower Carboniferous strata in the Marsel block has been restricted. This study establishes a regional high-frequency stratigraphic framework, identifies local microfacies and microfacies associations, and provides new interpretations of sedimentary environments of the Lower Carboniferous strata, thereby providing an improved basis for hydrocarbon exploration.

Geological setting and stratigraphy

The Early Carboniferous (Mississippian) was a time of changing global climate, sea level, and oceanic circulation as well as faunal abundance and diversity (Berner 1991; Mora et al 1996; Webb 2002). This time was marked by unstable icehouse conditions with fluctuating climate and multiple short-lived glaciations (Brand 1993; Kammer and Ausich 2006; Mullins and Servais 2008; Lowry et al. 2014). During the Late Devonian through Middle Carboniferous (Bashkirian), the Chu-Sarysu Basin was part of the passive continental margin of the western Kazakhstan plate with carbonate platforms mainly developed in the south of the basin (Cook et al. 1994, 2007). During the Early Carboniferous, the Kazakhstan plate was located at 10°–40°N where the climatic conditions were favorable for carbonate accumulation (Li and Jiang 2013), and limestone and siliciclastic mudstone with coals accumulated in the basin (IHS Energy Group 2012).

In the Marsel block, Lower Carboniferous strata of Tournaisian (C_1t), Visean (C_1v) and Serpukhovian (C_1sr) age are predominantly carbonate deposits with a top boundary of a regional overlap unconformity or disconformity and a bottom boundary of an overlap unconformity or truncation surface. The thickness of the Carboniferous strata is greater to the north, and paleotopography is inferred to have been lower to the north. Tournasian strata (C_1t) are 15–30 m thick, and consist of dark grey to black micritic limestone with thin beds of black mudstone. Visean strata are subdivided into three members with thicknesses of 100 m (C_1v-1), 120 m (C_1v-2), and 140 m (C_1v-3) respectively. The C_1v-1 member contains a large section of light grey to grey limestone with thin marl and gypsum beds, locally with thin beds of very fine grain sandstone. Dark grey marl and micritic limestone are developed in the lower part of C_1v-2 member and light grey packstones and grainstones are present in the upper part of C_1v-2 member in addition to pervasive dolostone. Dark micritic limestone and marl with thin beds of packstone and grainstone are present in C_1v-3 member. The C_1sr member has an average thickness of 210 m and is subdivided according to rock type into the following four vertical sections: (1) reef; (2) below reef; (3) evaporites; and (4) below evaporites. The "below reef" section includes marl and bioclastic wackestone. The "reef" section includes limestone with reef-framework bryozoans and coral, and reef-dwelling organisms such as brachiopods, gastropods and echinoderms. The “below evaporates” section includes bioclastic wackestone, packstone, and grainstone. The “evaporates” section includes gypsum and halite covering nearly the entire study area as a trap, interbedded with thin beds of limestone and dolostone.

Materials and methods

The data used in this study include more than 84 m of cores, geophysical well logs and images from 7 wells in the Marsel block, with about 300 thin sections from the cores. The sedimentary structures, depositional textures, grain types, and fossils were described by core observation and using a polarizing microscope. The content of argillites (siliciclastic mudstone) and different types of grains and fossils were estimated visually.

The classification of carbonate rocks follows the nomenclature of Dunham (1962), and the classification of sandstone compositions follows the nomenclature of McBride (1963). Standard microfacies and sedimentary models follow the work of Wilson (1975) and Flügel (2010), specifically with respect to microfacies identification, facies associations analysis, and sedimentary models of the Lower Carboniferous strata. For detailed sequence stratigraphic

interpretations, the Carboniferous-Permian sea-level curve of Haq and Schutter (2008) was consulted.

Depositional sequences

The Lower Carboniferous strata of the block can be divided into 4 depositional sequences and 18 parasequences on the basis of seismic, well-logging, and lithological data (Figs. 2, 3). The four depositional sequences can be roughly matched with C_1t—C_1v-1, C_1v-2, C_1v-3, and C_1sr. Each depositional sequence contains strata that are interpreted as a transgressive systems tract (TST), overlain by strata that are interpreted as a highstand systems tract (HST).

Depositional sequence 1 (SQ1) is composed of Tournaisian strata (black carbonate mudstone and marly limestone, mapped as C_1t) through lower Visean strata (limestone with marl and gypsum, mapped collectively as C_1v-1). SQ1 is approximately 115–130 m thick and lies immediately above Devonian siliciclastic strata. The contact of SQ1 with the underlying Devonian strata is an angular unconformity in the south, a parallel unconformity in the central part of the Marsel block, and is conformable in the north. In seismic data, the Devonian strata are characterized by medium to poor continuity seismic reflectors of weak amplitude, whereas the overlying strata of SQ1 are characterized by continuous seismic reflectors of strong amplitude (Fig. 2). The lower part of SQ1 (black carbonate mudstone and marly limestone, mapped as C_1t) is 10–30 m thick, and is interpreted as a TST, whereas the upper part of SQ1 (limestone with marl and gypsum, mapped collectively as C_1v-1) is 55–125 m thick, and is interpreted as a HST. The HST consists of a lower interval of 5–15 m-thick beds of gypsum, and an upper interval of grey medium-bedded to thick-bedded packstone/grainstone and dolomitic limestone with local beds of abundant bioclasts and intraclasts. Thin beds

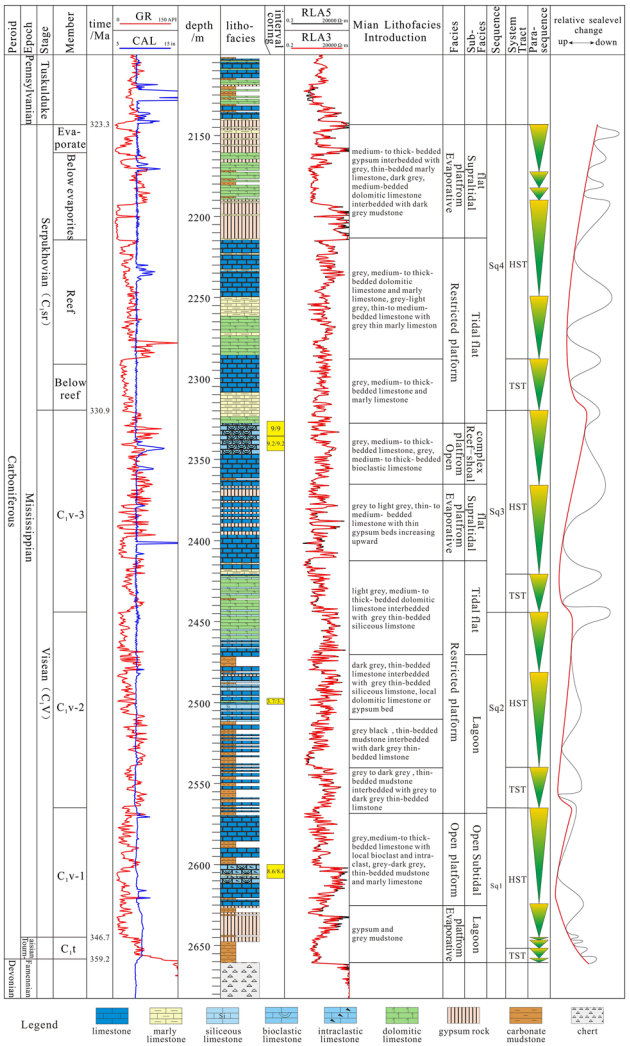

Fig. 3 Facies and sequence stratigraphy of Lower Carboniferous strata in Well ASSA-2 in the Marsel block

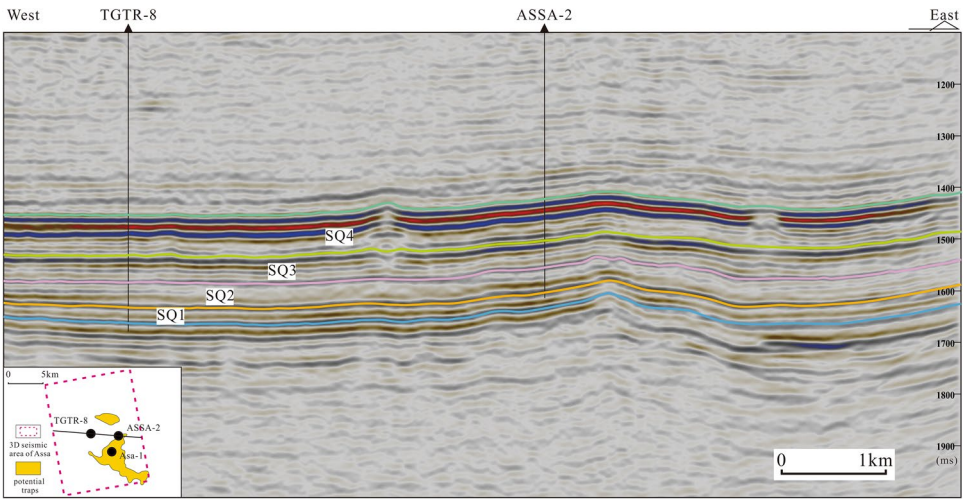

Fig. 2 Three-dimensional (3D) seismic profile showing the Lower Carboniferous depositional sequences (SQ1, SQ2, SQ3, SQ4) in the Marsel block of the Chu-Sarysu Basin

of grey to dark grey marly limestone and carbonate mudstone are present near the top of the HST. Gamma-ray (GR) geophysical logs of SQ1 generally show characteristics of gentle zigzag and a near-box shape on the whole, and its amplitude is from high to low due to the relatively higher content of marls in the lower part of SQ1 than those in the upper part of SQ1. These GR logs suggest that SQ1 may be subdivided into six parasequences (Fig. 4a). The lower four parasequences are of Tournaisian age and have relatively higher GR values, whereas the upper two parasequences are of Visean age and have relatively lower GR values with a typical stair-step shape. The resistivity logging curve is in the shape of box or bell, whereas the GR curve displays a relatively high amplitude with highly jagged edge. The lower two parasequences of SQ1 (black carbonate mudstone and marly limestone), which are considered to be the TST, are interpreted as restricted lagoon deposits. In contrast, the uppermost four parasequences of SQ1 (limestone with marl and gypsum) with an aggradational stack pattern, which are considered to be HST, are interpreted as evaporitic lagoon deposits. The uppermost two parasequences of SQ1 consist of thick-bedded gypsum overlain by deposits of dolomitic

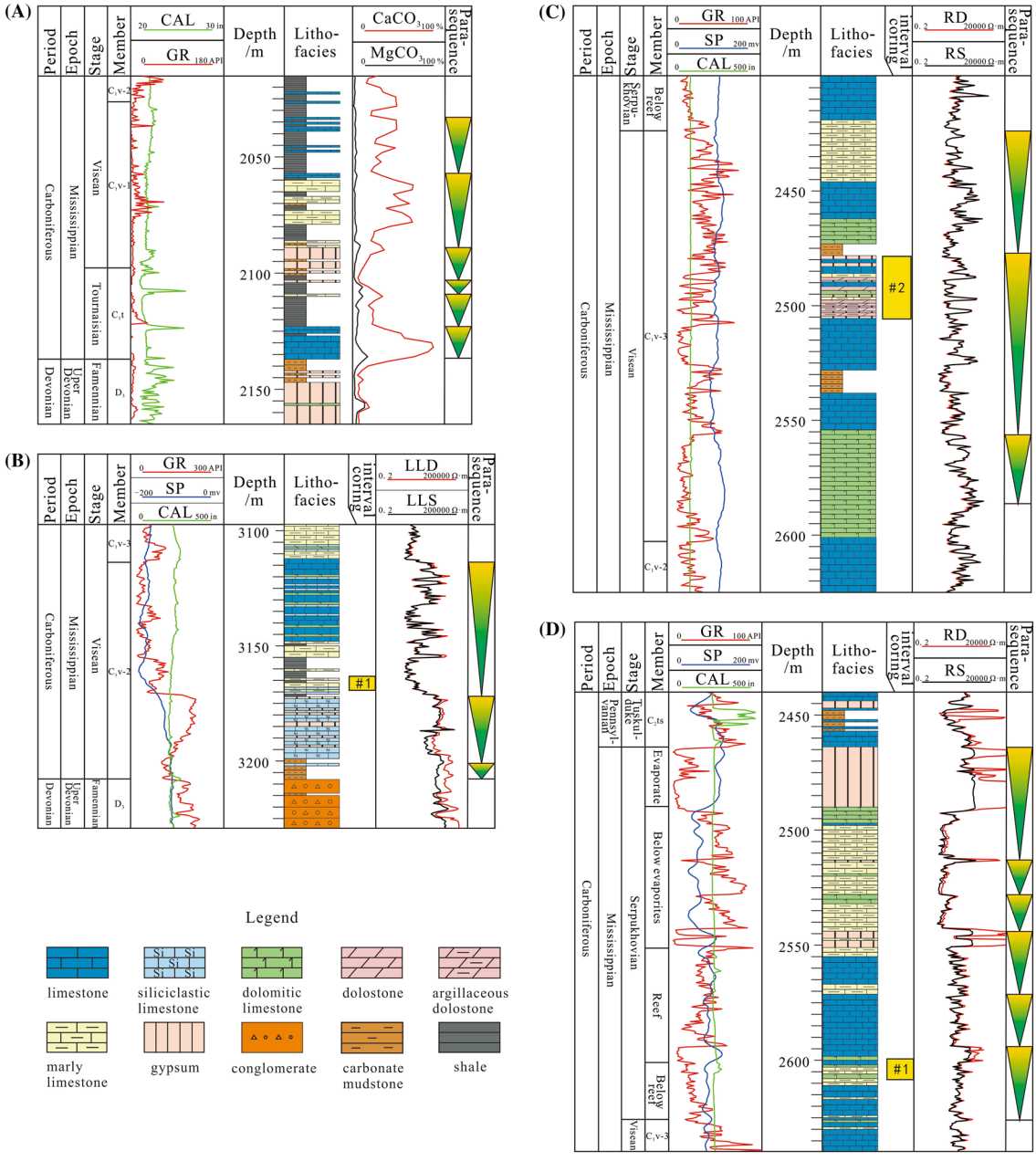

Fig. 4 Division and characteristics of parasequences in Lower Carboniferous strata in the Marsel block

limestone, bioclastic/intraclastic limestone interlayered with marly limestone/mudstone, or even dark grey to black shale indicating a strong TST. The upward increase in carbonate content is interpreted to indicate a relative rise in sea level (Fig. 4a).

Depositional sequence 2 (SQ2) is composed of middle Visean strata (a unit of dark grey marl and carbonate mudstone overlain by a unit of light grey dolomitic or siliceous limestone, mapped collectively as C_1v-2). SQ2 is approximately 120 m thick and lies immediately above SQ1. The contact of SQ2 with the underlying units of SQ1 is a parallel contact in seismic profiles of the Marsel block (Fig. 2) and it is interpreted as a sequence boundary based on the wireline log signature, lithofacies in wells and seismic data. In seismic data, the strata of SQ2 are characterized by seismic reflectors of medium energy, low to medium frequency, and medium continuity (Fig. 2). The lower part of SQ2 (dark grey marl, carbonate mudstone, and argillaceous limestone) is interpreted as a TST, whereas the upper part of SQ2 (light grey dolomitic or siliceous limestone) is interpreted as a HST. SQSQGR Geophysical gamma-ray logs of SQ2 show high values and a zigzag pattern in the TST (dark grey marl, carbonate mudstone, and argillaceous limestone), and a box shape in the HST (light grey dolomitic or siliceous limestone). These GR logs suggest that SQ2 may be subdivided into three parasequences (Fig. 4b). The upper boundary of each parasequence is characterized by the lower trending of the amplitude of GR curve and higher trending of zigzag of both GR and resistivity curves. The lower parasequence (dark grey marl, carbonate mudstone, and argillaceous limestone) corresponds to the TST of SQ2 and is interpreted as a restricted lagoon or low-energy marine bay deposits. The middle and upper parasequences (light grey dolomitic or siliceous limestone) correspond to the HST of SQ2 showing an aggradational stack pattern and are interpreted as restricted lagoon and tidal flat deposits. The occurrence of thin-beds of gypsum in the middle and upper parasequences suggests that the climate was probably hot and dry.

Depositional sequence 3 (SQ3) is composed of upper Visean strata (dark carbonate mudstone with beds of packstone and grainstone, mapped collectively as C_1v-3). SQ3 is approximately 140 m thick and lies immediately above SQ2. The contact of SQ3 with the underlying units of SQ2 is an obscure parallel contact in the seismic profiles of the Marsel block (Fig. 2) and it is interpreted as a sequence boundary based on the wireline log signature, lithofacies in wells and seismic data. In seismic data, the strata of SQ3 are characterized by seismic reflectors of low energy and medium to poor continuity (Fig. 2). The lower part of SQ3 (carbonate mudstone and marl) is interpreted as a TST, whereas the upper part of SQ3 (gypsum, packstone, and grainstone) is interpreted as a HST showing a retrogradational stack pattern on the whole (Fig. 4c). Gamma-ray (GR) geophysical logs of SQ3 show a zigzag pattern with gamma-ray values that increase upwards indicating a dirtying-up trend. On the basis of changes in both lithofacies and shape of GR curve, SQ3 is subdivided into three parasequences (Fig. 4c). The lower parasequence (carbonate mudstone and marl) corresponds to the TST of SQ3, and is interpreted as restricted lagoon and tidal flat deposits. The middle and upper parasequences correspond to the HST of SQ3. The middle parasequence (gypsum) is interpreted as evaporite flat (sabkha) deposits. The upper parasequence (light grey packstone and grainstone) is interpreted as shallow shoal deposits. The enhancing frequency and amplitude of the GR curve suggest a probable evolution in the frequency and amplitude of sea-level oscillation possibly caused by late Visean changes in climate such as those described by Wright and Vanstone (2001).

Depositional sequence 4 (SQ4) is composed of Serpukhovian strata, which consist of a unit of marl and bioclastic wackestone; overlain by a unit of reef-bearing boundstone; which in turn is overlain by a unit of wackestone, packstone, and grainstone; then overlain by a unit of gypsum and halite (all mapped collectively as C_1sr). SQ4 is approximately 160–340 m thick and lies immediately above SQ3. The contact of SQ4 with the underlying units of SQ3 is a parallel contact in the seismic profiles of the Marsel block (Fig. 2) and it is interpreted as a sequence boundary based on the wireline log signature, lithofacies in wells and seismic data. In seismic data, the strata of SQ4 are characterized by parallel seismic reflectors of good continuity and strong amplitude, with local areas of weak amplitude chaotic reflectors that are interpreted as bioherms (Fig. 2). The lowest unit of SQ4 (marl and bioclastic wackestone) is interpreted as a TST, whereas the overlying units of SQ4 (reef-bearing boundstone; overlying wackestone, packstone, and grainstone; and overlying gypsum) are interpreted as a HST. On the basis of lithological and GR curve features, six parasequences are recognized (Fig. 4d). The first and lowest parasequence (marl and bioclastic mudstone) corresponds to the TST of SQ4, and it shows low GR values overall in the shape of a funnel indicating a cleaning-up trend. It is interpreted as sub-tidal deposits. The second to the sixth parasequence corresponds to the HST of SQ4 showing a progradational stack pattern on the whole (Fig. 4d). The second and next lowest parasequence (reef-bearing boundstone) has a flatter GR log pattern in a reef box-shape and is interpreted as reef deposits. The third parasequence (wackestone, packstone, and grainstone) is characterized by a series of regional evaporitic deposits at the top and is interpreted as restricted and evaporite flat deposits formed after cessation of reef growth. The fourth to the highest parasequence (carbonate mudstone, dolomitic limestone or dolostone with gypsum interlayers) shows an even flattener shape of

the GR curve and lower GR values, and is interpreted as evaporite flat (sabkha) deposits.

Microfacies analysis

The Lower Carboniferous strata in the Marsel block contain carbonate lithofacies composed of a large variety of skeletal and non-skeletal grains, carbonate mudstone (micrite), calcite cements, and early diagenetic dolomite, with the presence of evaporites and mixed carbonate-siliciclastic deposits. The dominant skeletal grains are brachiopods, echinoderms (echinoids and crinoids), benthic foraminifera, ostracods, bryozoans, calcareous algae, gastropods, and sponge spicules, respectively. Non-skeletal grains are abundant and include ooids, intraclasts, peloids, grain aggregates, coated grains, and in some instances, detrital quartz silt/fine sand grains. Primarily on the basis of the lithology, sedimentary features, textures and fossil contents from rock specimens and thin sections, 20 microfacies (Mf) are distinguished for facies analysis of the Lower Carboniferous strata in the study area (Figs. 5, 6). These microfacies are grouped into four main facies associations. These microfacies and facies associations are briefly described below.

Microfacies characteristics and environment interpretation

Mf1 and Mf2 are both dark grey carbonate mudstone containing less than 10% bioclasts of brachiopods, echinoderms (echinoids and crinoids), benthic foraminifera, and ostracods. Mf1 contains a minor amount of ooids except above bioclasts and nodular fabrics with irregular shape (Fig. 5(1)).

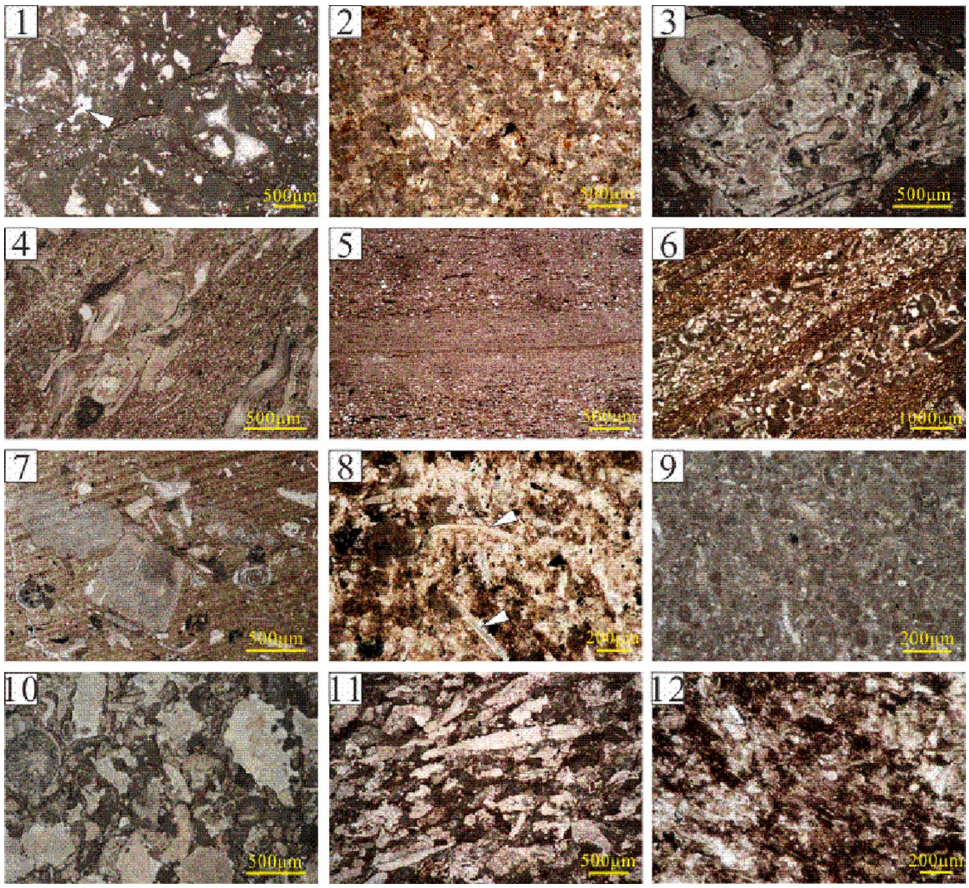

Fig. 5 Photographs of microfacies: **1** lime mudstone (Mf1); note the irregular nodular fabric and biological burrow in the lime mud matrix (arrow), well PRDS-18; **2** lime mudstone (Mf2), well ASSA-2; **3** bioclastic wackestone (Mf3), bioclastic clump, well KNDK-6; **4** bioclastic wackestone with terrigenous clay and silt (Mf3); note the bioclasts of echinoderms and brachiopods with oriented arrangement, well KNDK-6; **5** laminated terrigenous wackestone (Mf4), well ASSA-2; **6** laminated terrigenous clastic wackestone; note the interbeds of siliciclastic clasts and intraclastic and bioclastic grainstone or packstone (Mf4), well ASSA-2; **7** brachiopod and echinoderm floatstone with marl (Mf5), well KNDK-6; **8** sponge spicule wackestone; note the sponge spicules (arrows) (Mf6), well TMSK-1; **9** non-laminated intraclastic packstone (Mf7), well TGTR-1; **10** bioclastic packstone (Mf8), well PRDS-18; **11** argillaceous bioclastic packstone (Mf9), well ASSA-2; **12** algal bioclastic packstone (Mf10), well ASSA-2

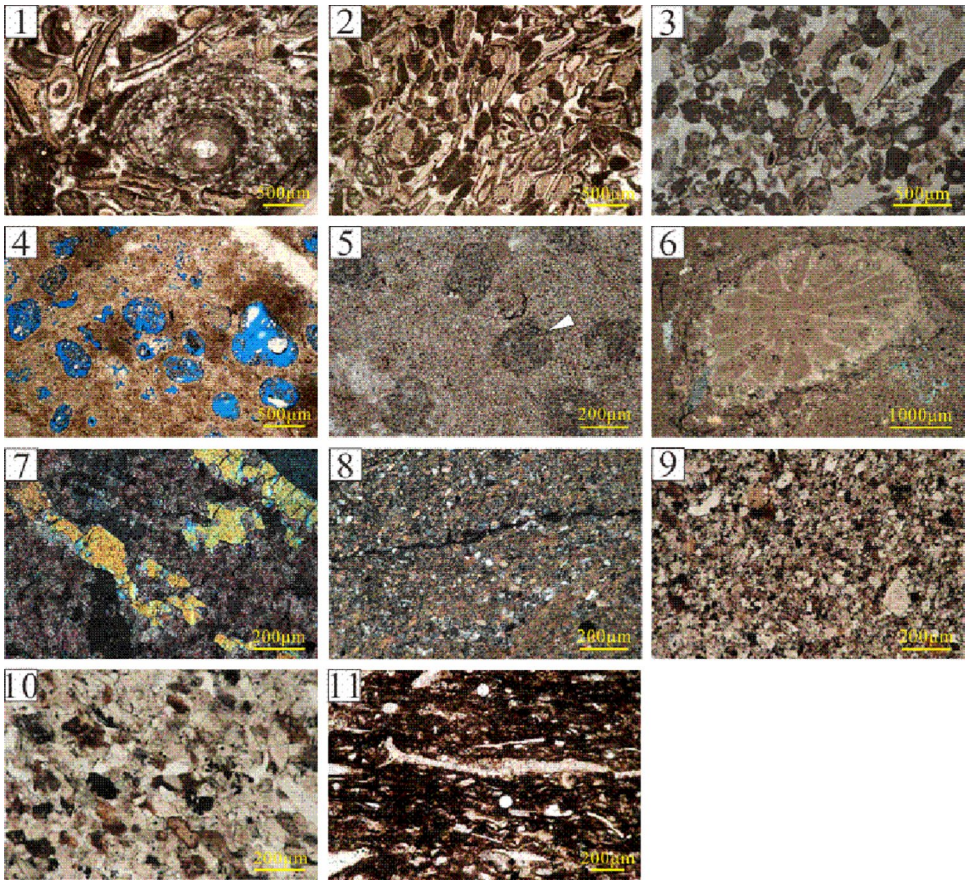

Fig. 6 Photographs of microfacies: **1** coated algal-bioclastic grainstone (Mf11), well ASSA-2; **2** oolitic grainstone (Mf12), well ASSA-2; **3** composite particle grainstone with sand-sized intraclasts, ooids, and bioclasts (Mf13), well PRDS-18; **4** bioclast-intraclast grain dolostone; note the mouldic pores (Mf14), well KNDK-6; **5** crystalline dolostone with replacement remnant texture (Mf15), note the original grain apparition (arrow), well KNDK-6; **6** bioclastic crystalline dolostone with corals replaced by gypsum (Mf15), well KNDK-6; **7** crystalline dolomitic limestone with anhydrite (Mf16), well TGTR-6; **8** grey feldspar siltstone (Mf17), well KNDK-6; **9** argillaceous siltstone (Mf18), well KNDK-6; **10** feldspathic litharenite siltstone (Mf19), well KNDK-6; **11** siliceous bioclastic shale (Mf20), well TMSK-1

Obvious biological burrows in the lime mud matrix and pressure dissolution stylolites are also developed. Mf1 can be correlated with the Ramp Microfacies (RMF) Type 2 of Flügel, formed on the outer ramp where the water energy is very low (Flügel 2010). Mf2 is characterized by a high content of clay up to 20% and well developed moldic porosity and body cavities with siliceous fillings (Fig. 5(2)), which is analogous to Standard Microfacies (SMF) Type 23 of Wilson (1975). This microfacies type suggests low-energy depositional conditions of a restricted platform or lagoon (Flügel 2010).

Mf3 to Mf6 are laminated bioclastic/intraclastic wackestone with a small amount of detrital terrigenous clasts. Mf3 is grey to dark grey bioclastic wackestone with local terrigenous clays, silts, or carbonaceous fragments (Fig. 5(3, 4)). The well-preserved bioclasts include echinoderms and brachiopods with oriented alignment, and a few bryozoans and ostracods. Some bioclasts are present in the shape of strips or clumps or mixed with silt-sized intraclasts as a conglomeratic aggregation. Laminar marl and sporadic pyrite are developed in thin section samples. Compared with SMF9 of Wilson (1975), it is considered that this microfacies formed in shallow lagoons with open circulation at or just below the fair-weathered wave base (FWWB). Mf4 is grey laminated terrigenous wackestone composed mainly of siliciclastic clasts (10–25%) of euhedral-granular silty fine-grained detrital quartz and argillaceous nodules (Fig. 5(5, 6)). Mf4 is also characterized by laminations consisting of siliciclastic clasts and layers of grainstone or packstone with intraclasts and bioclasts, representing possible storm deposits. On the basis of the above features, it is presumed that this microfacies is probably formed in the peritidal zone dominated by tidal currents and storms from the subtidal carbonate factory in the vicinity of the coast; and the paucity of bioclast debris indicates relatively restricted low-energy conditions. Mf5 is grey brachiopod and echinoderm floatstone with the marl content of 13% and bioclast content of about 40% including brachiopods, echinoderms, and very minor amounts of bryozoans and ostracods (Fig. 5(7)). Brachiopod and echinoderm (mainly crinoid stems and arm plates) fragments are embedded within a bioclastic wackestone matrix with fine laminations. It is likely that most accumulations of brachiopods and echinoderms occurred in mid-ramp settings similar to SMF12 of Wilson (1975). Mf6 is a dark grey sponge spicule wackestone (Fig. 5(8)). The predominant components of this microfacies are siliceous sponge spicules (~46%). The abundant matrix of carbonate mudstone (micritic) and very fine-grained texture suggest a low-energy environment below the fair-weather wave base and probably below storm wave base (SWB) similar to RMF1 of Flügel (2010).

Mf7 to Mf10 are packstone with various grains, such as skeletal fragments of echinoderms, brachiopods, bryozoans, ostracods, silt/sand-sized intraclasts, and ooids. Each microfacies has a distinctive type of grain combination representing different depositional conditions. Mf7 is grey to dark grey non-laminated intraclastic packstone with about 60% intraclasts and 11% bioclasts associated with strong silicification, including echinoderms (3%), brachiopods (3%), sponge spicules (3%), and bryozoans (2%) (Fig. 5(9)). The predominant silt-sized intraclasts are moderately sorted, subrounded to rounded, and silicified incompletely. In addition, the rock is locally bioturbated and strongly burrowed. Mf7 can be correlated with SMF16 of Wilson (1975) and is common in shallow platform interiors comprising protected shallow-marine environments with moderate water circulation and in inner ramp settings. Mf8 is a grey bioclastic packstone with about 50% bioclasts of echinoderms and brachiopods, 15% intraclasts, and 15% ooids (Fig. 5(10)). Particles show concavo-convex contact and suture contact and partial silicification. Well-developed pressure dissolution stylolites are filled with argillites and bitumens, and pervasive deformed or broken particles imply a strong diagenesis of compaction. Analogous to RMF14 of Flügel (2010), this microfacies indicates a near-shoal open inner ramp environment. Mf9 is dark grey argillaceous bioclastic packstone. Biofabric combinations of echinoderms (40%), brachiopods (20%)/ostracods (25%), bryozoans (30%) and brachiopods (25%) are the most common in this microfacies (Fig. 5(11)). Moreover, the microfacies is characterized by abundant organic mud (15–20%) and locally preferred bioclast orientation. Pyrite, carbonaceous fabric, and trace amounts of gypsum are also present locally. In addition, the inner parts or the rims of bioclastic particles are often silicified and somewhat recrystallized. From the above features, the microfacies is presumed to have formed in evaporitic lagoons corresponding to SMF16 described by Wilson. Mf10 is dark grey algal bioclastic packstone (Fig. 5(12)). This microfacies is characterized by the presence of calcareous algae (20%) and echinoderms (20%), with minor amounts of ostracods (5%), bryozoans (5%), sponge spicules (5%) and foraminifera (2%). Siliceous materials are present in the interparticle space as silts or have filled in the body cavity as silicification products. Similar to RMF7 by Flügel (2010), this microfacies represents restricted and low-energy inner ramp conditions, likely the euphotic shallow upper part of the subtidal zone that is favorable for calcareous algae.

Mf11-Mf14 are grey to dark grey grainstone in which the principle particles are skeletal debris of brachiopods, echinoderms (echinoids and crinoids), benthic foraminifera, ostracods, bryozoans, calcareous algae, and gastropods, as well as allochems of ooids, intraclasts, peloids, grain aggregates, and coated grains. Mf11 is a coated bioclastic grainstone with sparry cement including calcareous algae (15–35%) and bioclasts of brachiopods (25–35%) and echinoderms/foraminifera (25–35%)/ostracods (10–15%), as main constituents of grains, and minor aggregate grains (5%) and peloids (5%) (Fig. 6(1)). This microfacies is characterized by pervasive coating and locally various mineral replacement. Most bioclasts have dark micritic envelopes and some are concentrated and distributed randomly. The replacement and silicification of anhydrite and gypsum are common. The content of unevenly distributed anhydrite, replacive of in situ gypsum crystals, can reach up to 20% of this microfacies. The prevalence of cortoids indicate open, photic and well-agitated depositional settings, such as winnowed platform edge sands and reefs as described in SMF11 by Wilson (1975), whereas the presence of evaporitic minerals indicates climate change from warm and humid to hot and dry. Mf12 is an oolitic grainstone containing abundant (40–75%) moderate- to well-sorted, well rounded, sub-spherical to subelongate, radial ooids, with mean size of 0.2 mm, as well as a small percentage of silt-sized intraclasts (30%) or bioclasts (10–15%) of echinoderms, brachiopods, bryozoans, and gastropods (Fig. 6(2)). The ooid nuclei often consist of small bioclasts of foraminifera and sandy intraclast/algae/echinoderms. As a whole, the grains show point and line contact. In accordance with the SMF15 described by Wilson (1975) and Flügel (2010). This microfacies is interpreted as deposits under moderate to low-energy conditions usually in sea-marginal environments with elevated or lowered salinities. Many of these ooids originate in restricted environments, like lagoons or lagoonal ponds. Mf13 is a composite particle grainstone with a high grain content of 55–80% and various types of particle combination, such as silt-sized intraclasts (25–50%) and bioclasts (10–30%); sand-sized intraclasts (15–50%), ooids (5–30%), and bioclasts; bioclasts and sand-sized intraclasts; and ooids and silt-sized intraclasts (Fig. 6(3)). Apart from the above dominant particles, a tiny amount of algal aggregates (2–5%), algal clasts (2%), peloids (5–10%) and a few pellets are included. The particles exhibit laminar accumulation locally and point and line contact overall. In detail, the silt-sized intraclasts are moderate- to fine-sorted and oblate- to lath-shaped; the sand-sized intraclasts are moderate-sorted and sub-angular-shaped; the ooids are mainly deformed, superficial and synthesized/compound with a nucleus of intraclasts and foraminifera. The bioclasts are abundant including partially silicified brachiopods (5–10%), ostracods (5%), benthic foraminifera (5–15%), and echinoderms (5–10%), and often present in the form of combination of brachiopods and ostracods/foraminifera; foraminifera and echinoderms; ostracods, echinoderms and foraminifera. Furthermore, the facies is characterized by microorganism burrows, well-developed current bedding, and slight recrystallization. In summary, the microfacies suggests subtidal shoal conditions where the water current remained agitated near the platform margin. Mf14

is a grey bioclast-intraclast grain dolostone with replacement remnant texture generally accompanied by gypsum (15–20%) (Fig. 6(4)). Sand-sized intraclasts and bioclasts of brachiopods and echinoderms are the primary particles with the content of 40–50% and 10–20%, respectively, and are present within euhedral to subhedral crystalline dolomite. Residual intercrystalline pores and intragranular pores are well developed, although some intragranular pores are partly or fully filled with gypsum or anhydrite. Locally, Mf14 exhibits gypsums that fill in open and enlarged dissolved fissures or fractures. This microfacies is interpreted to have formed as a result of both sediment accumulation in subtidal to upper mid-ramp environments similar to RMF8 of Flügel (2010) and early diagenesis of dolomitization and dissolution.

Mf15 and Mf16 are grey crystalline dolostone or dolostone associated with tabular or needle-shaped gypsum/anhydrite. The dolomite crystals are euhedral to subhedral and micritic to silt-sized. In addition, the two microfacies are characterized by intercrystalline dissolved pores filled with gypsum or needle anhydrite aggregations. Mf15 is a bioclastic crystalline dolostone with remnant replacement texture (Fig. 6 (5) and (6)). The presence of original grain and matrix apparitions in euhedral to subhedral, micritic to silt-sized dolomite crystals and the presence of some fragments (10%) of corals and ostracods replaced by gypsum may suggest upper intertidal to lower supratidal environments with a slight water movement. Apart from that, recrystallized micritic dolomite, impregnated bitumen, and degypsumization are locally present. Mf16 is a crystalline dolomitic limestone or lime dolostone with unevenly distributed tabular anhydrites (15%) and minor gypsum (5%) (Fig. 6(7)). The lack of skeletal fragments, the euhedral and micritic dolomite accompanied by nodular anhydrite showing enterolithic and chicken-wire or fenestral structure, and the bird's-eye structure suggests accumulation in an evaporitic supratidal environment.

Mf17 to Mf19 are light-colored siliciclastic fine sandstone, siltstone, argillaceous siltstone, and silty mudstone with wavy, flaser and lenticular bedding (typical of tidal flat condition) and low-angle wedge-shaped cross bedding, which can be interpreted as inner to upper mid-ramp deposits dominated by the wave. Mf17 is a grey feldspar siltstone with silt accumulated in stripes or clumps (Fig. 6(8)). Pyrite, semi-open to open fractures and dissolved fissures are also present. Mf18 is a grey to dark-grey argillaceous siltstone or silty mudstone (Fig. 6(9)). The shale content usually varies between 25 and 40% (but attains 75% at some locations); the silt content usually varies between 60 and 70% (but attains 25% at some locations); and the pyrite content is approximately 5%. In argillaceous siltstones, a small amount of very fine-grain sand and locally concentrated pyrite is present; whereas, in silty mudstone, silt and pyrite are evenly distributed in mud matrix. Mf19 is light grey to grey feldspathic litharenite siltstone (Fig. 6(10)). The main mineral constituents are quartz (18%), feldspar (20%), detritus (mainly tuff, 50–60%) and pyrites (5%). The quartz grains are euhedral and semi-euhedral with the interference color of yellowish-white. All clasts are moderate to fine sorted, subangular to angular, with point and line contact, porous to mosaic cementation, and arranged in a preferred orientation. Furthermore, blocky calcite cement is present unevenly in the grain-supported rock; and pyrite is locally present in lamination and in clusters.

Mf20 is a dark grey argillaceous bioclastic shale (Fig. 6(11)). Mf20 consists of a large amount of clay (53%), silica (13%), bioclasts (35%), and minor detrital clasts (2%). The predominant fragments include ostracods (19%) and brachiopods (6%), a few echinoderms (3%) and bryozoans (3%), sponge spicules (3%) and trilobites (1%), all of the fragments showing a preferred orientation. Horizontal bedding is present, and some of the bioclasts show evidence of recrystallization and silicification. The above features lead to an interpretation of a mid- to outer ramp depositional environment.

Microfacies associations characteristics

Seven types of microfacies associations (MA1–MA7) were identified on the basis of microfacies stacking patterns that reflect correlative environments. Each association represents a distinct facies succession organized within a parasequence.

MA1 (Mf9–Mf11–Mf10–Mf13) is present in the middle part of C_1v-1 and is interpreted as having accumulated in relatively restricted low-energy conditions in well ASSA-2 in the north-central part of the Marsel block. Both the gamma-ray curve and the relative dolomite content curve associated with MA1 are very straight and smooth with very low gamma-ray values (10–15 API units) and relative dolomite content logging near zero (Fig. 7a). MA1 mainly includes grey to dark grey grainstone and packstone with dominant calcareous algae and bioclasts of echinoderms and ostracods arranged in a preferred orientation. In addition, horizontal bedding in the lower succession and low-angle wedge-shaped cross bedding in the upper succession show a shallowing-upward trend, interpreted to represent an increase in energy toward the top. The deposits were probably controlled by gentle wave current near wave base or accumulated in a lower subtidal photic zone.

MA2 (Mf1–Mf6–Mf20–Mf9) is present in the middle part of C_1v-2 in well TMSK-1 in the northwestern part of the Marsel block. The shape of gamma-ray curve associated with MA2 is more zigzag than that of MA1 because the curve has a little wider range of values (60–80 API units). The relative dolomite content curve has jagged edges with the logging values increasing upward (< 0.4)

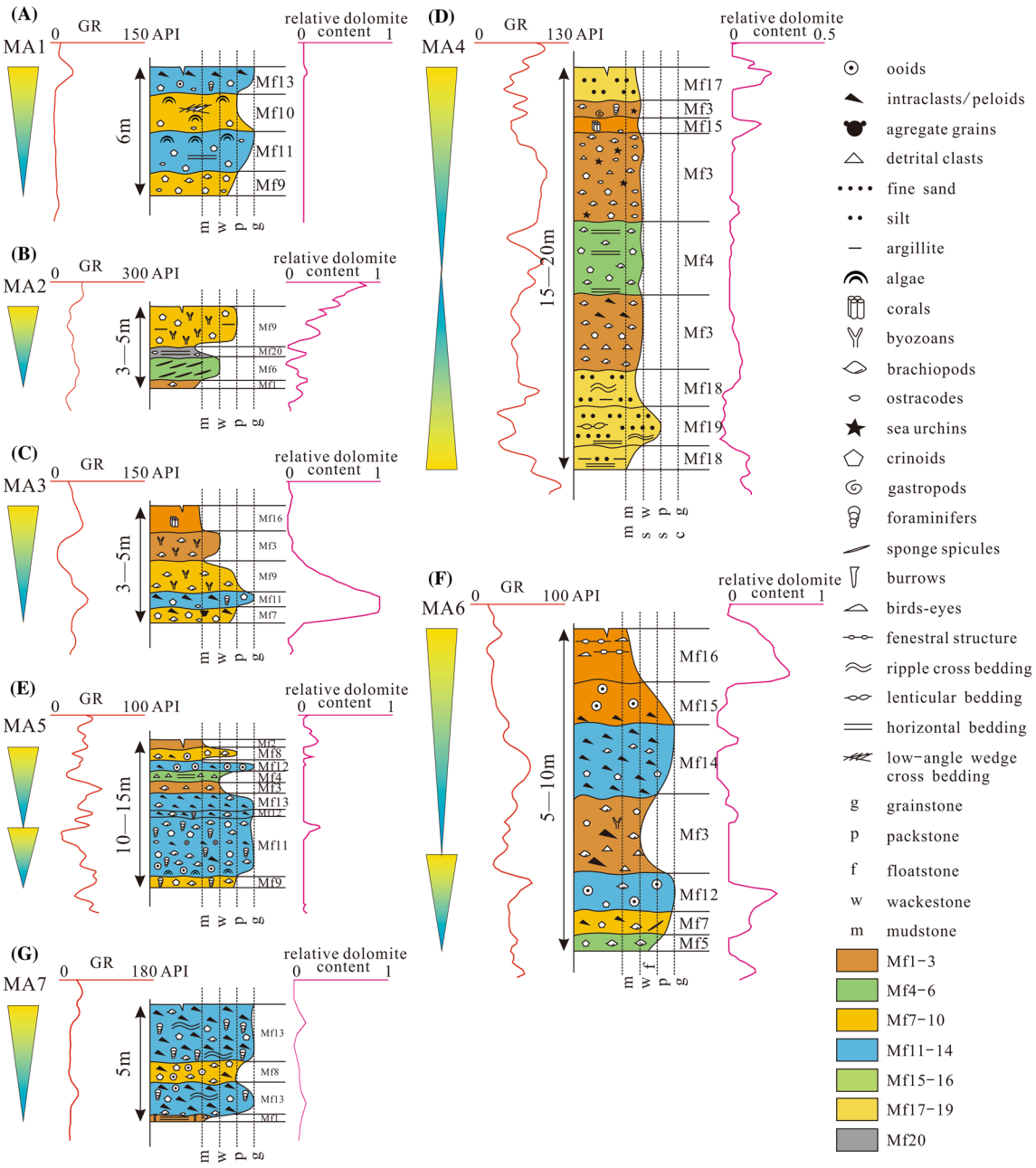

Fig. 7 Microfacies associations recognized in Lower Carboniferous strata in the Marsel block

(Fig. 7b). Lithofacies of MA2 vary from dark grey lime mudstone rich in organic matter (Mf1) and dark grey sponge spicule wackestone (Mf6) to dark grey siliceous bioclastic shale (Mf20) and dark grey to dark grey argillaceous bioclastic packstone (Mf9). The proportion of bioclasts of bryozoans, ostracods, and echinoderms increases toward the top, and this trend suggests that the hydrodynamic conditions became stronger. Additionally, these characteristics suggest that sufficient current existed to orient the skeletal fragments in shale and packstone with common carbonaceous fragments. In general, this microfacies association is interpreted to represent a change of depositional setting from an outer ramp to an evaporitic lagoonal environment.

MA3 (Mf7–Mf11–Mf9–Mf3–Mf16) is present in the middle part of C_1v-2 in well ASSA-2. The shape of the gamma-ray curve associated with MA3 is a funnel with a wider range of values (10–50 API units) and gentle edges (Fig. 7c). The box-shape relative dolomite content curve indicates the likely dolomitization of the lower succession.

The microfacies types are vertically arranged in (regressive) shallowing-upward successions consisting of grey to dark grey non-laminated intraclastic packstone with local bioturbation and strong burrowing (Mf7), interpreted as restricted lagoonal sediments that accumulated near an inner ramp; coated algal-bioclastic grainstone (Mf11), interpreted as subtidal high-energy deposits, and dark grey to dark grey argillaceous bioclastic packstone (Mf9), interpreted as low-energy lagoonal deposits; dark grey wackestone overlain by grey to dark grey bioclastic wackestone with local terrigenous clay, silt, or carbonaceous fragments (Mf3), interpreted as subtidal to lower intertidal deposits, and very fine crystalline dolostone with remnant replacement texture (Mf16), interpreted as supratidal deposits. The abundance of bioclasts in packstone composed of echinoderms and brachiopods is obviously lower (10–20%) than that in grainstone (60–70%) mainly consisting of echinoderms, ostracods, and foraminifera.

MA4 (Mf18–Mf19–Mf9–Mf3–Mf4–Mf3–Mf16–Mf3–Mf17) is present in the middle and upper C_1v-3 and upper C_1sr units in well KNDK-6 in the northeastern Marsel block. MA4 consists of a lower unit of grey to light grey siliciclastic strata including fine sandstone, siltstone, argillaceous siltstone, and silty mudstone with tidal beddings; a middle unit of grey to dark grey carbonate strata including argillaceous bioclastic packstone, bioclastic wackestone, and brachiopod and echinoderm floatstone; and an upper unit of grey to light grey siliciclastic strata that are similar to the lower unit of MA4. The shape of the MA4 gamma-ray curve displays both relatively frequent changes in the lower and upper siliciclastic units, and the curve is smoother in the middle carbonate unit, with an average value of 20 API units. The relative dolomite content curve shows changes close to the boundary corresponding to the alternation of detrital siliciclastics and carbonates (Fig. 7d). The vertical stacking pattern of these microfacies is interpreted as reflecting the change in depositional setting from a nearshore subtidal to intertidal environment, to a restricted evaporitic lagoon on a carbonate platform interior and a shallow lagoon with good current circulation in the middle to lower part of a middle ramp as a result of relative sea rise; then a change to upper intertidal to a lower supratidal environment with mild current agitation; and finally to a superatidal environment on the platform interior as a record of relative sea fall.

MA5 (Mf9–Mf11–Mf12–Mf13–Mf5–Mf3–Mf12–Mf8–Mf2) is present near the top unit of C_1v-3 in well ASSA-2. MA5 is characterized by sedimentation patterns of several meters to decimeter grainstone, including coated algal-bioclastic grainstone (Mf11), oolitic grainstone (Mf12), and composite particle grainstone (Mf13), interpreted as having accumulated in subtidal conditions. This succession is overlain by units of bioclastic wackestone (Mf3) and brachiopod and echinoderm floatstone (Mf5), interpreted as having accumulated below fair-weather wave base or even storm wave base due to sea-level rise, regularly punctuated by prominent unconformities in bioclastic packstone (Mf8), interpreted as exposure surfaces that developed on a near-shoal open inner ramp deposits caused by sea-level fall, and subsequently overlain by thin-bedded carbonate mudstone (Mf2) interpreted as having accumulated during an abrupt change to deeper-water of a restricted platform (Fig. 7e). The shape of the MA4 gamma-ray curve is a combination of a tunnel and a Christmas tree shape from bottom to top; and the relative dolomite content curve is basically flat with locally minor fluctuations (Fig. 7e). In similar strata of the Mid-continent in the United States, such increasingly frequent cyclic lithofacies changes between grainstone/packstone and wackestone/mudstone and the expanding variation of particle size in limestones of different lithofacies are interpreted to reflect progressive increase in both the frequency and the amplitude of the glacio-eustatic sea-level oscillations (Smith and Read 2000). Such cyclic stratigraphic patterns are thought to represent Milankovitch eccentricity effects (Horbury 1989; Vanstone 1996) and are associated with the onset of glacio-eustatic changes during the late Visean (Wright and Vanstone 2001).

MA6 (Mf7–Mf12–Mf4–Mf3–Mf14–Mf16–Mf15) is present in the lower and upper C_1sr units occupying most of the northern Marsel block. The gamma-ray curve associated with MA6 is Christmas tree shaped in the lower part and funnel-shaped in the upper part with a wide range of values (30–65 API units). The relative dolomite content curve is funnel-shaped at the bottom and bell-shaped at the top (Fig. 7f). The non-laminated intraclastic packstone (Mf7) and oolitic grainstone (Mf12) present in the lower C_1sr unit are interpreted as having accumulated under low- to moderate-energy restricted platform setting with carbonate sand shoals and are interpreted the same as the laminated terrigenous wackestone (Mf4) formed in the subtidal conditions. The appearance of bioclastic wackestone (Mf3) marks of the start of another cycle, is considered as deposits in the open marine zone below fair-weather wave base resulting from relative sea-level rise. The cycle ends with beds of bioclast-intraclast grain dolostone (Mf14), bioclastic crystalline dolostone with remnant replacement texture (Mf15), and crystalline dolomitic limestone or lime dolostone with evaporites, which have typical depositional structures of evaporitic peritidal environments. In summary, MA6 comprises several microfacies of cyclic deposits formed in low- to moderate-energy conditions on a restricted platform at first, and then in the open marine waters below fair-weather wave base, and lastly in an evaporitic platform.

MA7 (Mf1–Mf13–Mf8–Mf13) is present in the middle C_1sr unit in well PRDS-18 in the southeastern part of the Marsel block. MA7 is interpreted as having accumulated under low- to moderate- energy conditions and in environments ranging from outer ramp to shallow shoal and near-shoal open middle ramp. The shape of the MA7 gamma-ray curve has little fluctuation with a narrow value range of 20–30 API units and the relative dolomite content curve

exhibits a slightly increasing trend in Mf13 (Fig. 7g). The dark grey thin-bedded carbonate mudstone (Mf1) with bioturbation structures and horizontal bedding at the bottom is interpreted as outer ramp deposits. The overlying thick-bedded composite particle grainstone (Mf13) indicates that the depositional setting changed into a moderate-energy subtidal shoal environment. The presence of interbedded grey bioclastic packstone (Mf8) implies a near-shoal open inner ramp environment. Hence, MA7 strata accumulated in a broad range of open marine environment on both outer and inner ramps.

Facies correlation and sedimentary models

Sedimentary facies and parasequences of Lower Carboniferous strata in SQ1-SQ4 are correlated with wells TMSK-1, TGTR-6, ASSA-2, and KNDK-6 (Fig. 8), located in the northern part of the Marsel block where potential reservoirs of shallow patch shoals are present. The vertical stacking patterns and lateral distribution of facies are different across the area. Furthermore, both facies maps for SQ1 to SQ4 (Fig. 9) and a sedimentary model (Fig. 10) for the integrated Lower Carboniferous strata are proposed for the Marsel block on the basis of the variation of microfacies, their corresponding associations, and facies correlation. The Lower Carboniferous strata are thought to have accumulated in a passive continental margin ramp environment and all the microfacies and their associations are grouped into the following six major facies belts: outer ramp, restricted lagoon in middle ramp, shallow shoal in inner ramp, restricted lagoon in inner ramp, subtidal to intertidal in inner ramp, and supratidal in inner ramp (Fig. 10).

The TST of SQ1 is only about 5–10 m thick, and the facies in the TST of SQ1 are dominated by dark-colored mud, shale, and lime mudstone, locally interbedded with or capped by evaporiticlagoon deposits of gypsum (interpreted as restricted lagoon deposits) in northeastern area. The HST of SQ1 contains five parasequences and is dominated by limestone, marly limestone and carbonate mudstone. In ASSA-2 well, the HST of SQ1 is primarily characterized by successive units of packstone and grainstone (MA1), whereas in wells TGTR-6 and KNDK-6 the succession consists mainly of carbonate mudstone (interpreted as tidal flat deposits). These features indicate that restricted low-energy shallow shoals were present in the area of the ASSA-2 well.

The TST of SQ2 is only about 10 m thick and is composed of carbonate mudstone and thin-bedded gypsum, overlain by thin-bedded carbonate mudstone. The HST of SQ2 contains two parasequences. The lower part of the HST in well TMSK-1 is composed of successive units of carbonate mudstone, siliceous bioclastic shale, and argillaceous packstone (MA2) that are interpreted as outer ramp to a restricted subtidal lagoon deposits up to the upper parasequence, similar to the stacking pattern in well TGTR-6. However, in well ASSA-2, the parasequences of the HST are dominated by successive units of packstone, argillaceous wackestone, and dolostone (MA3), interpreted as sediments that accumulated in low-energy lagoons near an inner ramp, subtidal high-energy shoals and shallower carbonate tidal flat in accordance with the regression successions. In addition, the HST of SQ2 in well KNDK-6 is characterized by thin-bedded limestone and interbedded thin-bedded carbonate mudstone, which are interpreted as having accumulated in a tidal flat environment.

The TST of SQ3 is about 10–100 m thick and is composed of successive units of marly limestone (interpreted as restricted lagoon deposits), dolomitic limestone, and carbonate mudstone (interpreted as sub-intertidal flat deposits). The HST of SQ3 is composed of two parasequences. The lower parasequence consists of limestone and marly limestone in the most northwestern area of the Marsel block and is capped by marker beds of regional evaporates. However, in well KNDK-6, the lower parasequence of the SQ3 HST is composed of successive units of (1) sandstone and siliciclastic mudstone, and (2) wackestone, packstone, and floatstone (MA4), interpreted as sediments that accumulated in a nearshore detrital tidal flat environment to a lagoonal environment associated with evaporite deposits as sea-level rose, and to a superatidal environment on the platform interior as sea-level fell. Hence, in summary, the lower parasequence of the HST of SQ3 is interpreted as restricted to semi-restricted lagoon deposits in the most northwestern area and mixed tidal flat in the northeast. The upper parasequence of the SQ3 HST is composed of limestone and marly limestone that is interpreted as restricted lagoon deposits in the northwest area and sub-intertidal flat deposits toward the east. It is noteworthy that in well ASSA-2, the top of the upper parasequence of the SQ3 HST is composed of successive units of carbonate mudstone, wackestone, packstone, grainstone, and floatstone (MA5), interpreted as sediments that accumulated in subtidal shoals to near-shoal as the platform interiors jumped into an even deeper and restricted environment.

The TST of SQ4 is about 20–30 m thick and composed of dark grey thin- to medium-bedded marly limestone or carbonate mudstone that is thought to have accumulated in a restricted environment during a rapid transgression. The HST of SQ4 is composed of five parasequences. They are successive units of wackestone, grain dolostone, lime dolostone with evaporites, crystalline dolostone with remnant replacement texture, and dolomitic limestone (MA6), which are interpreted as sediments that accumulated on a restricted and evaporitic platform. It is notable that two regionally correlated sections of evaporites are developed in the middle and top of the HST separately, showing that there are at least two large-scaled cycles of obvious

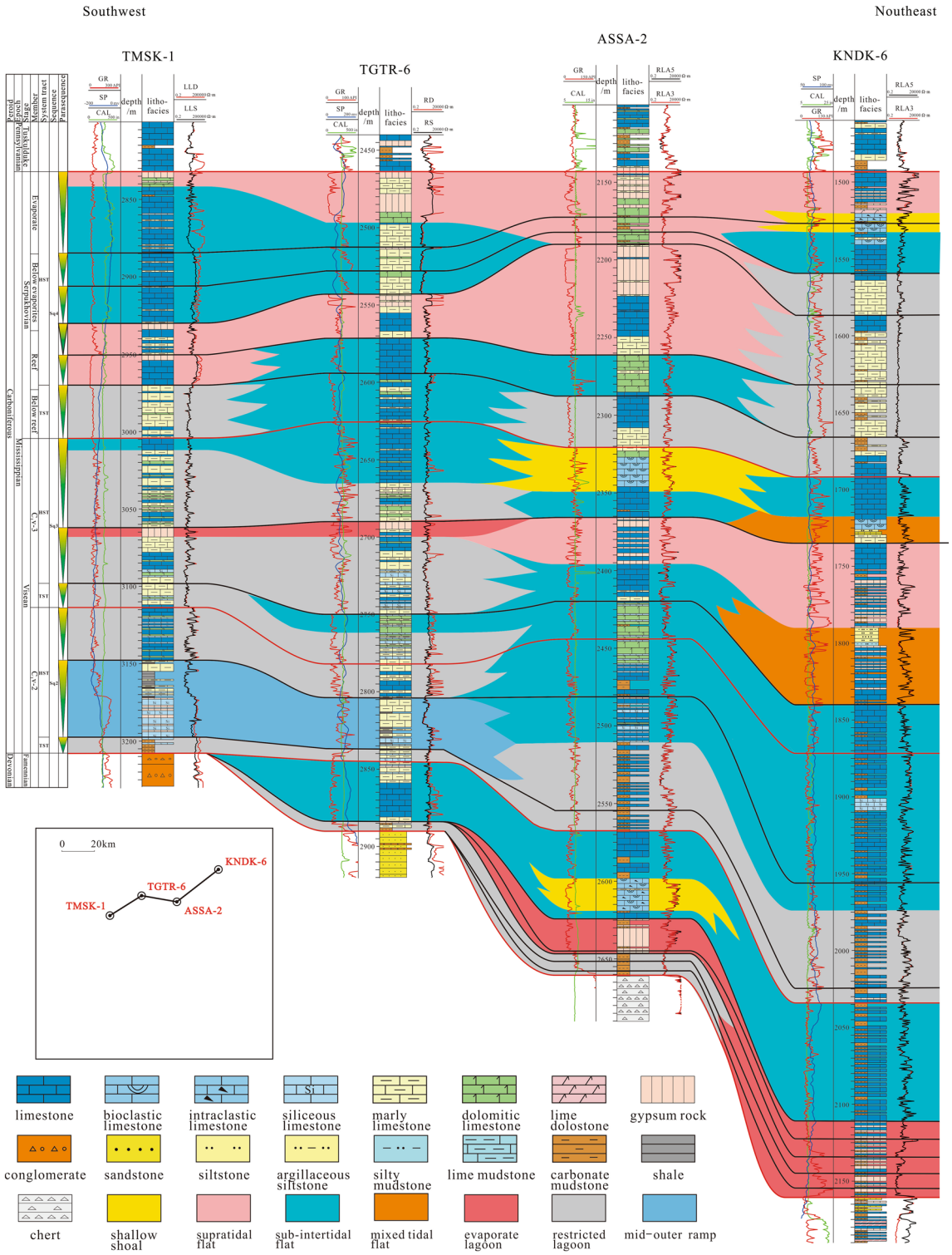

Fig. 8 Sedimentary facies and parasequence correlation in Lower Carboniferous in the Marsel block

regression, which ended with MA6. In addition, in well PRDS-18, the successive units of dark grey thin-bedded carbonate mudstone, overlain by thick-bedded composite particle grainstone and interbedded grey bioclastic packstone (MA7), are interpreted as the outer ramp, subtidal shoal, and near-shoal inner ramp deposits.

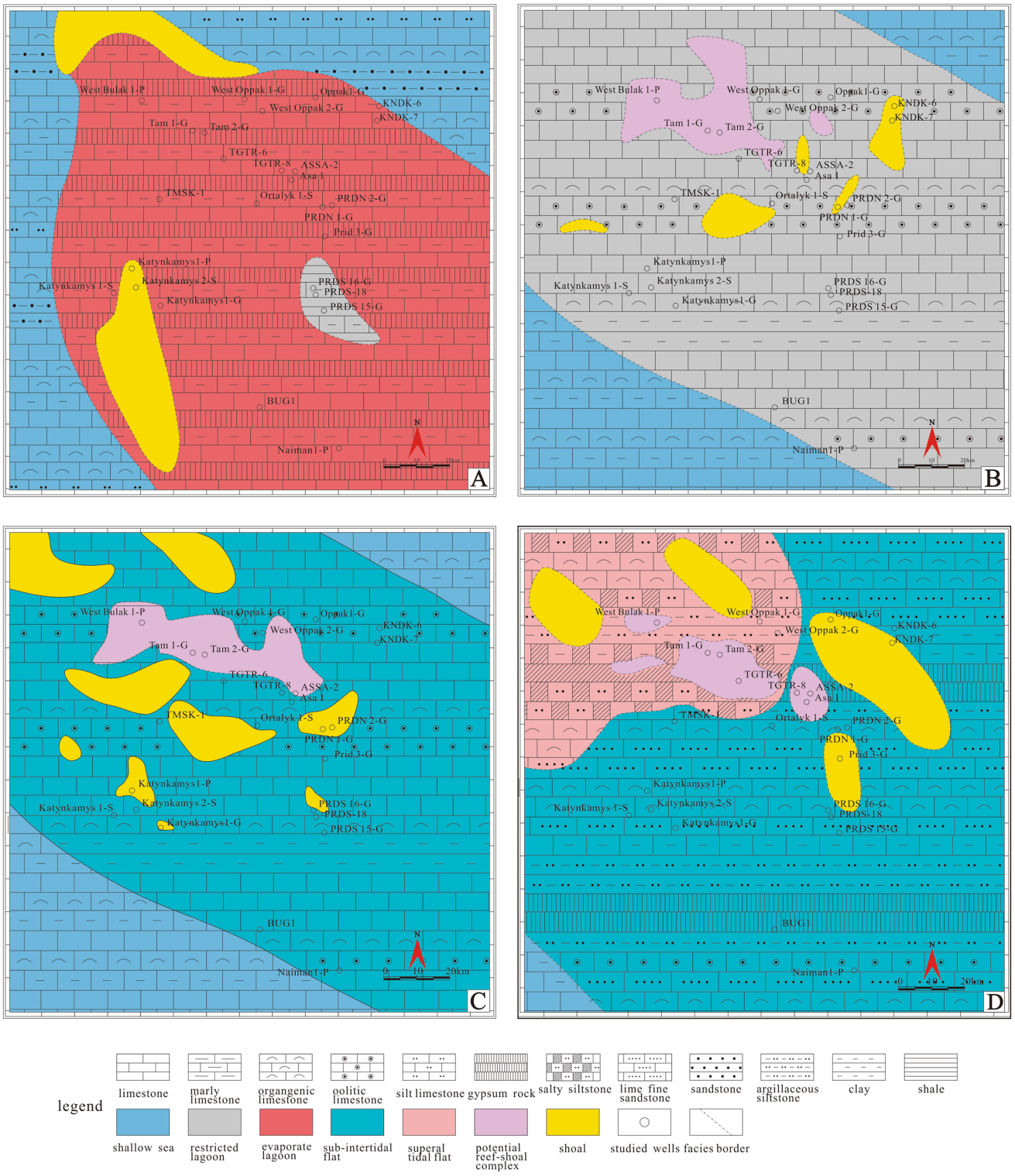

Fig. 9 Facies maps of SQ1–SQ4 in the Lower Carboniferous strata in the Marsel block

Discussion

Previous studies have suggested that the Serpukhovian reef and shoal complexes identified in seismic profile serve as the premier hydrocarbon reservoir in the northern part of the Marsel block (Xu et al. 2014; Pang et al. 2014). In this study, several micritic coral reefs are present in Mf16 in the upper parasequence of the HST of both SQ2 and SQ4, indicating

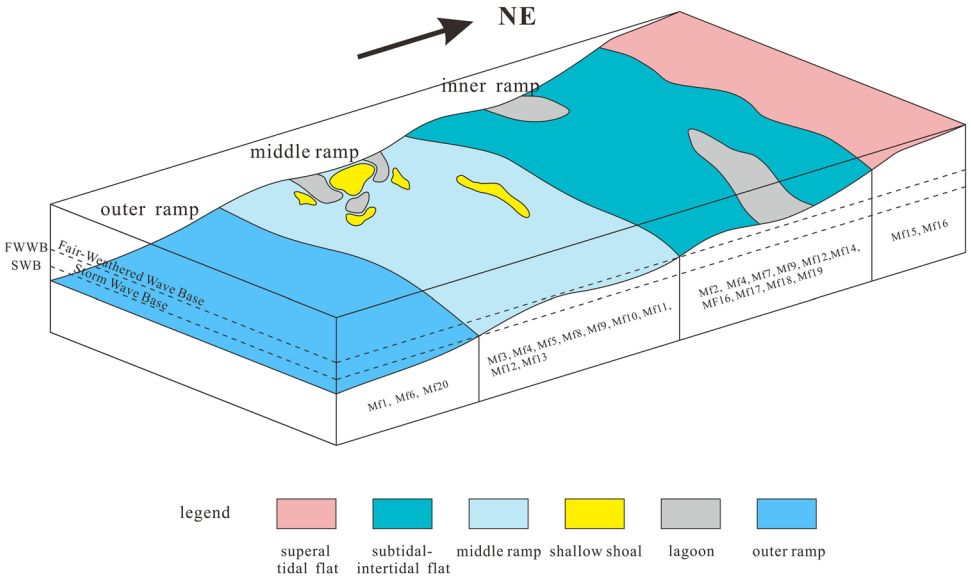

Fig. 10 Depositional model of Lower Carboniferous strata in the Marsel block

the existence of corals and enhancing the possibility of reef framework construction. In addition, compared with other shoal deposits in the north-central part and south-eastern part of the platform interiors, the widespread prevailing dissolution of aragonitic grains and bioclasts in Mf16 in the upper parasequence of the HST of SQ4, also has produced considerable moldic and intra-granular porosity in favorable reservoirs developed in a narrow zone near the shoreline of a typical coastal sabkha. According to Yechieli and Wood (2002), the porosity development is probably due to meteoric diagenesis of early dissolution and dolomitization, as well as the contribution of seawater to the solute budget, depending on the ratio of the width of the supratidal zone to the total width.

During the Early Carboniferous, the Marsel block was located in the center of the Eurasian continent at around 30°N, in the subtropical high-pressure zone associated with arid subaerial or shallow-marine conditions favorable for the formation of carbonate platforms (Scotese 2002; Abrajevitch et al. 2008; Abadi et al. 2017). The end-Devonian faunal extinction event and the extreme global warming during the Early Carboniferous inhibited reefal growth (Webb 2002; Aretz and Chevaliers 2007; Shen and Qing 2010), and thus enhanced the development of an extensive carbonate ramp. Furthermore, the widespread limestone, dolomitic limestone (interpreted as tidal flat deposits) and abundant micrites in all microfacies also indicate a carbonate ramp environment for the Lower Carboniferous in the Marsel block. In addition, the four occurrences of regional evaporates are indicators of dry and warm climate conditions. Such climate events, associated with glacial-interglacial cyclicity and tectonic activity, are known from other studies to have occurred during the Early Carboniferous (Isbell et al. 2003; Haq and Schutter 2008; Fröhlich et al. 2010), and such changes are also thought to have affected the Marsel block during the Lower Carboniferous.

Conclusions

This publication uses data from cores, thin sections, and well logs data in order to describe and interpret the Lower Carboniferous strata in the Marsel block of Chu-Sarysu Basin in southern Kazakstan. The conclusions are summarized as follows:

(1) Four depositional sequences, each composed of transgressive systems tract (TST) and highstand systems tract (HST), were delineated in the Lower Carboniferous strata, These sequences roughly coincide, respectively, with the following four stratigraphic intervals (1) lower Tournasian (C_1t) through lower Visean (C_1v-1); (2) middle Visean (C_1v-2) strata; (3) upper Visean (C_1v-3) strata; and (4) Serpukhovian (C_1sr) strata. Furthermore, these depositional sequences can be subdivided into 18 parasequences bounded by instantaneous drowned punctuated surface (C_1t and C_1v) or instantaneous exposed punctuated surface (C_1sr).

(2) Twenty microfacies (Mf1–Mf20) were identified within the Lower Carboniferous strata of the Marsel block in the Chu-Sarysu Basin. These microfacies are distinguished by textures, structures, grains (types, sizes, and sorting), fossil types and abundance, and argillaceous content. Each type of microfacies reflects a specific depositional environment with a certain level of current energy.

(3) Seven microfacies associations (MA1–MA7) were used to group specific ordered microfacies successions

developed within a parasequence. Each microfacies association is organized in a single shallowing-upward high-frequency sequence or a composite one consisting of two shallowing-upward high-frequency sequences or a deepening-upward high-frequency sequence combined with a shallowing-upward one, representing variations among different depositional facies, such as outer ramp (Mf1, Mf6, Mf20), mid ramp (Mf5), restricted lagoon (Mf2, Mf12), shallow lagoon with open circulation (Mf3), evaporitic lagoon (Mf9), carbonate and evaporitic tidal flat (Mf4, Mf7, MF8, Mf10, Mf11, Mf16), mixed tidal flat (Mf17–Mf19) in the platform interiors, and carbonate sand shoal (Mf13–Mf15) on an open platform.

The depositional environment for the Lower Carboniferous strata is a classic carbonate ramp, which is characterized by vast covering of inner ramp facies, including tidal flat (MA1, MA3, MA5), lagoon (MA4) and patch shoals (MA6, MA7) developed in the northern and southeastern part of the platform, whereas middle and outer ramp facies (MA2) occupy a relatively small area. The HST deposits of late Visean and Serpukhovian composed of grainstone, grain dolostone, and bioclastic crystalline dolostone with remnant replacement texture (interpreted as carbonate sand shoal or shallow shoal deposits) in the northern and southeastern part of the platform are of the best quality for petroleum reservoirs.

Acknowledgements Funding for this project was kindly provided by the Geo-jade Petroleum Corporation, Beijing, China. We really appreciate it for providing substantial well and seismic data and financial support. The authors also would like to thank the School of Energy Resources, China University of Geosciences, China, for providing laboratory and equipment for polarizing and CL Photomicrographs of thin sections; the Laboratory Experiment and Test Institute of Xinjiang Oilfield Corporation affiliated to China National Petroleum Corporation for help in rock type description and fossil identification.

Funding Funding was provided by the National Basic Research Program of China (973 Program) (Grant No. 2011CB201100-03) and also Fundmental Research Funds for the Central Universities of China (Grant No. 2652015362).

References

Abadi MS, Kulagina EI, Voeten DFAE, Boulvain F, Silva ACD (2017) Sedimentologic and paleoclimatic reconstructions of carbonate factory evolution in the Alborz Basin (northern Iran) indicate a global response to Early Carboniferous (Tournaisian) glaciations. Sediment Geol 348:19–36

Abrajevitch A, Voo RVD, Bazhenov ML, Levashova NM, Mccausland PJA (2008) The role of the Kazakhstan orocline in the late Paleozoic amalgamation of Eurasia. Tectonophysics 455:61–76

Aretz M, Chevaliers E (2007) After the collapse of stromatoporid-coral reefs-the Famennian and Dinantian reefs of Belgium: much more than Waulsortian mounds. Geol Soc Spec Publ 275:163–188

Berner RA (1991) A model for atmospheric CO_2 over phanerozoic time. Am J Sci 65:685–694

Brand U (1993) Global perspective of famennian-tournaisian oceanography: geochemical analysis of brachiopods. Ann Soc Géol Belg 115:491–496

Cook HE, Zhemchuzhnikov VG, Buvtyshkin VM, Golub LY, Gatovsky YA, Zorin AY (1994) Devonian and Carboniferous passive-margin carbonate platform of Southern Kazakhstan: summary of depositional and stratigraphic models to assist in the exploration and production of coeval giant Carbonate platform oil and gas fields in the North Caspian Basin, Western Kazakhstan. In: Embry AF, Beauchamp B, Glass DJ (eds) Pangea: global environments and resources. Canadian Society of Petroleum Geologists, Calgary, pp 363–381

Cook HE, Zhemchuzhnikov VG, Zempolich WG, Lehmann PJ, Alexeiev DV, Zhalmina VY, Zorin AY (2007) Devonian and Carboniferous carbonate platform facies in the Bolshoi Karatau, southern Kazakhstan: outcrop analogs for coeval carbonate oil and gas fields in the North Caspian basin oil and gas of the Greater Caspian area. AAPG Stud Geol 55:159–163

Dunham RJ (1962) Classification of carbonates rocks according to depositional texture. Mem Am Assoc Petrol Geol 1:108–121

Effimoff I (2001) Future hydrocarbon potential of Kazakhstan. AAPG Mem 74:243–258

Flügel E (2010) Microfacies of carbonate rocks. Springer, Berlin, pp 657–723

Fröhlich S, Petitpierre L, Redfern J, Grech P, Bodin S (2010) Sedimentological and sequence stratigraphic analysis of Carboniferous deposits in western Libya: recording the sedimentary response of the northern Gondwana margin to climate and sea-level changes. J Afr Earth Sci 57:279–296

Haq BU, Schutter SR (2008) A chronology of Paleozoic sea-level changes. Science 322:64–68

Horbury AD (1989) The relative roles of tectonism and eustasy in the deposition of the Urswick Limestone in south Cumbria and north Lancashire. Research 6:153–169

IHS Energy Group (2012) International petroleum exploration and production database includes data current as of August. Database available from IHS Energy Group. IHS Energy Group, Chu-Sarysu Basin, Kazakhstan

Isbell JL, Miller MF, Wolfe KL, Lenaker PA (2003) Timing of late Paleozoic glaciation in Gondwana: was glaciation responsible for the development of Northern Hemisphere cyclothems? Spec Pap Geol Soc Am 370:5–24

Kammer TW, Ausich WI (2006) The "age of crinoids": a Mississippian biodiversity spike coincident with widespread carbonate ramps. Palaios 21:238–248

Li AB, Filip'Yev GP (1982) Prospects for discovery of new fields in Chu-Sarysuy basin. Pet Geol 20:132–133

Li JH, Jiang HF (2013) World Atlas of Paleoplate Reconstruction, Lithofacies Paleogeography and Paleoenvironment. Geological Publishing House, Bath, pp 65–67 **(in Chinese)**

Lowry DP, Poulsen CJ, Horton DE, Torsvik TH, Pollard D (2014) Thresholds for Paleozoic ice sheet initiation. Geology 42:627–630

McBride EF (1963) A classification of common sandstones. J Sediment Petrol 33:664–669

Mora CI, Driese SG, Colarusso LA (1996) Middle to late paleozoic atmospheric CO_2 levels from soil carbonate and organic matter. Science 271:11051107

Mullins GL, Servais T (2008) The diversity of the Carboniferous phytoplankton. Rev Palaeobot Palynol 149:29–49

Pang XQ, Huang HD, Lin CS, Zhu XM, Liao Y, Chen JF, Kang YS, Bai GP, Wu GD, Yu FS, Jiang FJ, Xu JL (2014) Formation,

distribution, exploration, and resource/reserve assessment of superimposed continuous gas field in Marsel block, Kazakhstan. Acta Pet Sin 35:1012–1056 **(in Chinese with English abstract)**

Pang XQ (2016) Genetic mechanism and prediction methodology for overstacked and continuous hydrocarbon accumulations. Science Press, Beijing **(in Chinese)**

Scotese CR (2002) Paleomap website. https://www.scotese.com, https://www.chris@scotese.com

Shen JW, Qing H (2010) Mississippian (Early Carboniferous) stromatolite mounds in a fore-reef slope setting, Laibin, Guangxi, South China. Int J Earth Sci 99:443–458

Sinitsyn FY (1991) Relationship of cyclicity of Lower Carboniferous gasproducing sediments to tectonic movements in the Chu Sarysu sineclise. J Petrol Geol 25:92–95

Smith LB, Read JF (2000) Rapid onset of late Palaeozoic glaciation on Gondwana: evidence from Upper Mississippian strata of the Mid-continent, United States. Geology 28:279–282

Sokolov BA, Dumnov YD, Lar'kova TN (1979) Evolution of the oil-gas prospects of the Chu-Sarysuy sedimentary basin. AAPG 16:376–379

Sokolova YA (1974) Secondary mineralization and oil potential of Lower Carboniferous rocks in Chu-Sarysu basin in relation to tectonic activity. Int Geol Rev 16:741–748

Vanstone SD (1996) The influence of climatic change on exposure surface development: a case study from the Late Dinantian of England and Wales. Geol Soc Spec Publ 107:281–301

Webb GE (2002) Latest Devonian and Early Carboniferous reefs: depressed reef building following the middle Paleozoic collapse. SEPM Spec Publ 72:239–269

Wilson JL (1975) Carbonate facies in geologic history. Springer, New York, pp 1–95

Wright VP, Vanstone SD (2001) Onset of Late Palaeozoic glacio-eustasy and the evolving climates of low latitude areas: a synthesis of current understanding. J Geol Soc Lond 158:579–582

Xu GF, Lin CS, Li ZT (2014) Lithofacies paleogeopraphy and favorable reservoir of Lower Carboniferous in southern Kazakhstan. J Northeast Pet Univ 38:1–11 **(in Chinese with English abstract)**

Yechieli Y, Wood WW (2002) Hydrogeologic processes in saline systems: playas, sabkhas, and saline lakes. Earth Sci Rev 58:343–365

Zheng JZ, Zhou HY, Huang XX (2009) Basic characteristics of petroleum geology and exploration potential analysis in Kazakhstan. China Pet Explor 14:80–86 **(in Chinese with English abstract)**

Affiliations

Yuan Wang[1,2] · Changsong Lin[3] · Yanda Sun[4] · Jingyan Liu[5] · Hao Li[3] · Haiquan He[4] · Qinglong Wang[4] · Muye Ji[3] · Manli Zhang[3] · Bozhi Zhao[3] · Zhiyuan Zhang[5]

[1] PetroChina Research Institute of Petroleum Exploration and Development, Beijing 100083, China

[2] Key Laboratory of Marine Reservoir Evolution and Hydrocarbon Enrichment Mechanism, Ministry of Education, Beijing 100083, China

[3] School of Ocean Sciences, China University of Geosciences (Beijing), Beijing 100083, China

[4] Geo-Jade Petroleum Corporation, Beijing 100016, China

[5] School of Energy Resources, China University of Geosciences (Beijing), Beijing 100083, China